Phonon Dispersion and Electron-Phonon Coupling in MgB_2 and AlB_2

K.-P. Bohnen, R. Heid, and B. Renker

Forschungszentrum Karlsruhe, Institut für Festkörperphysik, P.O.B. 3640, D-76021 Karlsruhe, Germany

(Received 15 March 2001)

We present a *first principles* investigation of the lattice dynamics and electron-phonon coupling of the superconductor MgB_2 and the isostructural AlB_2 within the framework of density functional perturbation theory using a mixed-basis pseudopotential method. Complete phonon dispersion curves and Eliashberg functions α^2F are calculated for both systems. The main differences are related to high frequency in-plane boron vibrations, which are strongly softened in MgB_2 and exhibit an exceptionally strong electron-phonon coupling. We also report on Raman measurements, which support the theoretical findings. Implications for the superconducting transition temperature are briefly discussed.

DOI: 10.1103/PhysRevLett.86.5771 PACS numbers: 74.70.Ad, 74.20.–z, 74.25.Kc

Recently, superconductivity has been observed in MgB_2 with an exceptionally high transition temperature for such a simple compound ($T_c \sim 39$ K) [1]. This system has in the mean time received a lot of attention from many experimentalists as well as theorists since understanding superconductivity in this binary compound should be much easier than in the high-T_c cuprate materials studied extensively for more than ten years now. This is due to the simpler lattice structure and the missing complication due to magnetism and strong electron-electron correlations. Already, early experiments [2–7] as well as theories [8,9] have suggested that we are dealing here with an s-wave superconductor based on strong electron-phonon coupling although alternative coupling mechanisms have also been discussed [10,11].

Modern band-structure calculations, together with *ab initio* determination of the phonon dispersion, electron-phonon coupling, and solution of the Eliashberg equations to calculate the transition temperature, should help one to understand the role played by the electron-phonon coupling in this material. Although recently many contributions have been published concerning the electronic band structure [8,9,12] only a few attempts have been made to proceed along the above-mentioned road map to a deeper understanding of the electron-phonon coupling. Most investigations are restricted to calculations of the phonon modes for the Γ point only [2,13]. Estimates of the coupling strength are therefore not very accurate, thus asking for a more complete treatment of the electron-phonon coupling in the whole Brillouin zone (BZ).

We have carried out such a systematic study of the lattice dynamics and the electron-phonon coupling using the mixed-basis pseudopotential method. To get a better understanding of the relevance of the electron-phonon mechanism we have studied two isostructural systems: MgB_2, which is superconducting, and AlB_2, for which no superconductivity has been found so far. This offers the possibility to compare the phonon dispersion curves to identify those which are strongly influenced by electron-phonon coupling even without calculating the coupling strength. Furthermore, the calculation of the Eliashberg function α^2F for both systems allows for a consistency check of the proposed phonon-mediated pairing mechanism.

Only very recently (after completion of our study) we became aware of a similar investigation by Kong *et al.* [14] which calculated the full phonon dispersion, the electron-phonon coupling, and T_c for MgB_2 within the linear muffin-tin orbital method. Our calculations are very similar to those presented in Ref. [14]; however, due to the parallel treatment of MgB_2 and AlB_2, they offer additional information.

In contrast to all other calculations presented so far we have structurally optimized both systems, thus we remain fully in the framework set by the theory. For comparison and checks of sensitivity of our results we have also studied certain phonon modes using the experimental structure. All our calculations are carried out using the mixed-basis pseudopotential method [15]. For Mg and Al we have used well-tested pseudopotentials of Martins-Troullier–type [16] and BHS-type [17]. The boron pseudopotential was constructed according to the Vanderbilt description [18] which led to a fairly deep p potential for the boron atom which, however, could be dealt with very efficiently due to the mixed-basis formulation. The wave functions were constructed from localized s and p functions at the Boron sites supplemented by plane waves with an energy cutoff of 16 Ry. Detailed tests were carried out to ensure convergence with respect to the number of plane waves as well as with respect to k-point sampling [19]. Different Monkhorst-Pack k-point sets have been used up to 13 824 k-points in the BZ together with a Gaussian smearing of 0.2 eV. The calculation of the phonon dispersion is based on a recently developed mixed-basis perturbation approach [20] which also allowed for the calculation of the electron-phonon coupling [21]. Finally, estimates of T_c are obtained by solving the linearized form of the Eliashberg equations [22]. Structural parameters were found to be fairly insensitive to the k-point sets while individual phonon modes were very sensitive to the sampling, thus pointing to strong electron-phonon coupling. All our calculations were carried out

TABLE I. Structural parameters of the optimized geometries. Experimental values (in brackets) are taken from Refs. [27,31].

	V (Å^3)	c/a	B (Mbar)
MgB_2	28.481 (29.010)	1.153 (1.142)	1.47 (1.20)
AlB_2	24.617 (25.578)	1.09 (1.084)	1.84

using the local exchange-correlation potential of Hedin and Lundqvist [23].

Since both systems crystallize in the so-called "AlB_2 structure" with alternating hexagonal (Mg, Al) layers and graphitelike B-layers, structural optimization required optimization of volume V and the c/a ratio. Table I gives calculated results for V and c/a as well as the bulk modulus B together with the experimental values. For both systems a slightly smaller volume has been found by the theoretical treatment compared to the experimental one. This is a typical behavior in local density approximation calculations. The c/a ratio is slightly larger. The electronic band structure obtained for MgB_2 is very similar to the ones obtained by other groups [8,9,24] with hole pockets around the Γ point extending along the Γ-A direction. AlB_2 has a very similar band structure; however, due to the additional electron density, no hole pockets around Γ and the Γ-A direction exist.

In Table II we have summarized our phonon results for the Γ point obtained from calculations based on the experimental structure as well as on the optimized one. With the exception of the E_{2g} mode (in-plane boron mode) all other modes are fairly insensitive to structural changes, as can be seen from Table II. The same also holds true for the sensitivity with respect to k-point sets. All previous calculations of the Γ-point phonon modes for MgB_2 agree very well with these results, with the exception of the E_{2g} mode, where shifts of ± 100 cm^{-1} have been observed [8,13,14]. As extensive studies have shown [19], this is mostly an effect of k-point sampling and indicates strong electron-phonon coupling for this mode. By comparing these results with those obtained for AlB_2, the most dramatic changes occur again for the E_{2g} mode, which stiffens substantially and becomes the highest one, and the B_{1g} mode (out-of-plane boron mode), which is strongly softened.

We have measured the E_{2g} mode by Raman scattering from samples of commercially available MgB_2 and AlB_2 powders. The samples showed clear x-ray diffraction patterns and consisted of crystalline grains up to 10 μm (MgB_2) and 50 μm (AlB_2). Measured spectra showed only one prominent line in agreement with space group P6/mmm and were not particularly polarization dependent. Typical results are presented in Fig. 1. The experimental result for AlB_2 is in almost perfect agreement with the calculated one. For MgB_2 the Raman line is very broad; however, the peak position agrees reasonably well with the calculated one while the linewidth is likely to be due to strong electron-phonon coupling (see discussion below).

TABLE II. Comparison of the calculated Γ-point phonon frequencies for the experimental (I) and optimized (II) geometries. Values are given in meV (cm^{-1}).

	MgB_2		AlB_2	
Mode	I	II	I	II
E_{1u}	39.9 (322)	40.5 (327)	33.0 (266)	36.6 (295)
A_{2u}	48.9 (394)	50.2 (405)	48.6 (392)	52.1 (420)
E_{2g}	66.5 (536)	70.8 (571)	118.3 (954)	125.0 (1008)
B_{1g}	86.3 (696)	87.0 (702)	59.9 (483)	61.3 (494)

Having studied carefully the Γ-point modes we also calculated the full phonon dispersion for both systems. Results are presented in Fig. 2 which were obtained by determining the dynamical matrix on a (6,6,6) reciprocal lattice grid in the hexagonal Brillouin zone. The results for MgB_2 agree very well with those of Ref. [14] and thus give additional credibility to the theoretical treatment.

By comparing the phonon density of states (DOS) shown in Fig. 2, certain features are worth mentioning. The biggest difference between the two systems shows up in the intermediate region of phonon frequencies where AlB_2 shows nearly a gap due to the strong dispersion of the relevant modes while, for MgB_2, this gap has nearly completely disappeared. High density of states at the upper and lower ends of the frequency range shows up in both systems. To compare with recent measurements by inelastic neutron scattering [25] we have also calculated the generalized density of states (weighted by the inelastic scattering cross section and the mass) broadened by a

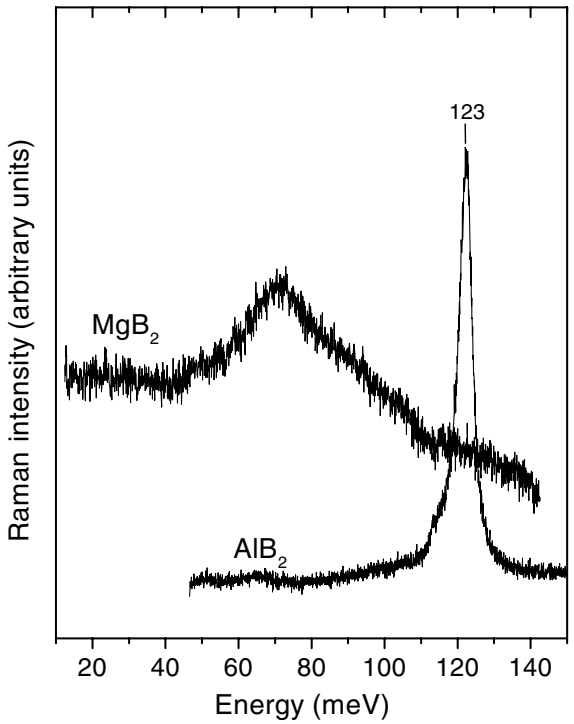

FIG. 1. Micro-Raman spectra obtained from polycrystalline grains of MgB_2 and AlB_2 at room temperature ($\lambda = 514.5$ nm).

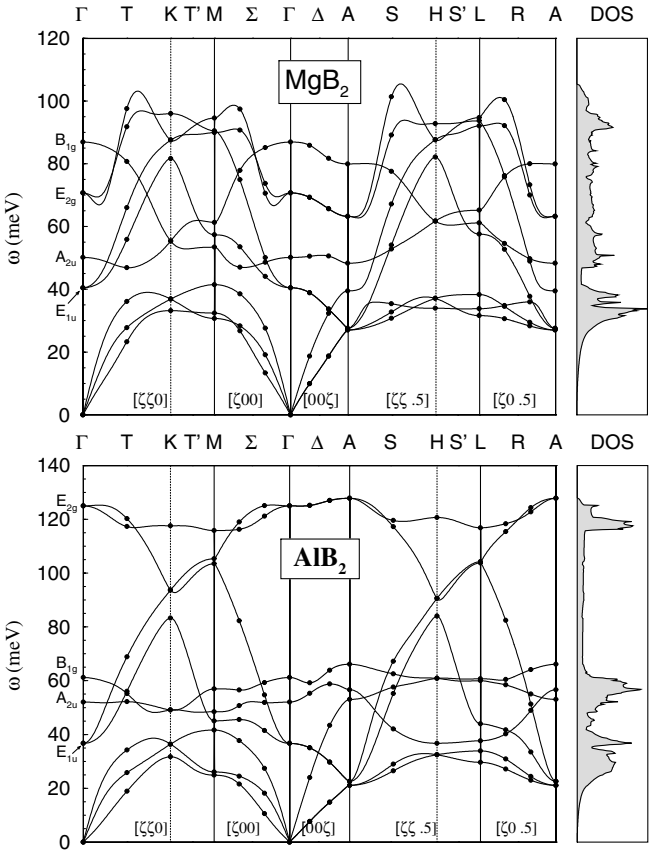

FIG. 2. Theoretical phonon dispersion curves along high-symmetry lines of the hexagonal BZ (notation after [32]) and DOS of MgB_2 and AlB_2. The dots represent actually calculated modes; lines are obtained by Fourier interpolation.

Gaussian with a width of 4 meV. The result in Fig. 3 should be compared directly with Fig. 1 in Ref. [25]. An almost perfect agreement with respect to peak positions, shoulders, and even with the relative ratio of contributions is obvious. We don't find any indication of a peak in the spectra near 17 meV, as observed by Sato *et al.* [26].

In the dispersion curves shown in Fig. 2, the layered structure of the crystals is reflected in a weak dispersion of the optical branches along Γ-A and in an anisotropy in the slopes of the acoustic branches, in agreement with experiments [27]. Besides many similarities, two very significant differences between AlB_2 and MgB_2 can be seen. The first one is related to the branches which evolve from the doubly degenerate E_{2g} mode at the Γ point. In MgB_2, these branches are strongly renormalized towards lower frequencies mostly near Γ and along the Γ-A direction. This is probably related to the hole pockets found in the electronic band structure of MgB_2 which are absent in AlB_2. The second distinctive difference is the behavior of branches starting from the B_{1g} mode, which in MgB_2 is significantly harder in certain regions of the BZ than in AlB_2.

To address the superconducting properties we have calculated the so-called Eliashberg function $\alpha^2F(\omega)$, using a

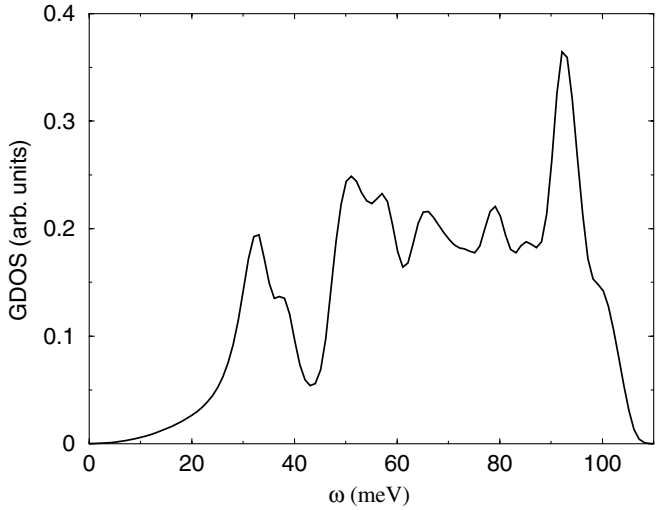

FIG. 3. Calculated generalized phonon density of states of MgB_2. Values for the incoherent scattering cross sections are taken from Ref. [25].

very fine (36,36,36) k-point grid in performing the Fermi-surface average of the electron-phonon matrix elements [28]. Results are presented in Fig. 4. For MgB_2 we find indeed a very large contribution to α^2F in the intermediate region between 60 and 70 meV, which is mainly due to strongly softened in-plane vibrations of the boron atoms as mentioned above. At Γ, for the E_{2g} mode, this strong coupling results in a very large linewidth of 15 meV in accordance with the broad feature seen in the Raman spectrum (Fig. 1). For AlB_2, in contrast, the biggest contributions show up at very high frequencies as well as in the regime of the acoustic modes; however, they are substantially smaller than the main contribution in MgB_2. From the Eliashberg function we calculate the electron-phonon coupling constant

$$\lambda = 2 \int_o^\infty d\omega \, \frac{\alpha^2 F(\omega)}{\omega}$$

which gives $\lambda_{MgB_2} = 0.73$ and $\lambda_{AlB_2} = 0.43$. For the logarithmically averaged phonon frequencies as defined in Ref. [14] we find 60.9 and 49.9 meV for MgB_2 and AlB_2, respectively. The values for MgB_2 agree well with the results of Ref. [14]. The fairly large value of λ for AlB_2, however, is unexpected.

Within the dirty limit of superconductivity [29] the calculation of the transition temperature T_c requires the knowledge of α^2F and the Coulomb pseudopotential μ^* [22]. As commonly done, we treat μ^* as an adjustable parameter. A T_c of 40 K for MgB_2 is obtained for $\mu^* = 0.05$. The same μ^* value leads to $T_c \sim 9$ K for the system AlB_2. This result is in contrast to the experimental situation, where no superconductivity has been found so far for AlB_2. There are basically two possibilities to reconcile the theoretical results with the experimental situation. One possibility is a different screening in AlB_2

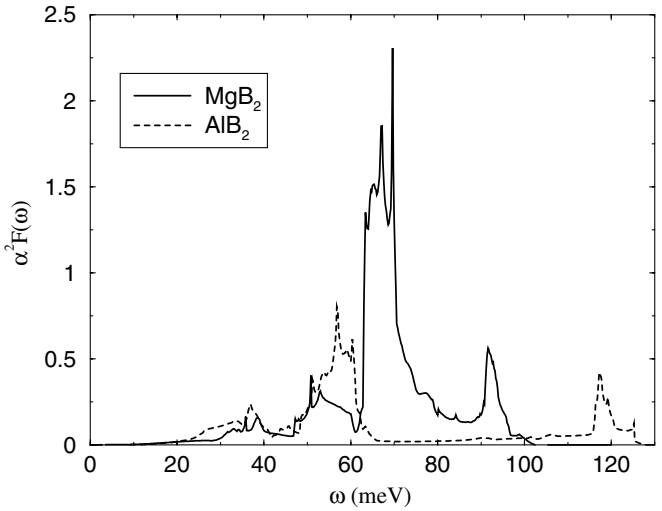

FIG. 4. Calculated Eliashberg functions $\alpha^2F(\omega)$ for MgB_2 and AlB_2.

compared to MgB_2 which has been speculated about in Ref. [30], leading to different values for μ^*. Alternatively, the approximation of an isotropic superconductor (dirty limit) might not hold. Because of the fact that we have dealt with both systems on equal footing, new questions have emerged which need further studies.

We have presented here first principles calculations of the phonon dispersion and electron-phonon coupling for two systems MgB_2 and AlB_2 which crystallize in the same lattice structure, but which have fairly different phonon dispersion curves. These results are in excellent agreement with measured quantities. The calculation of the superconducting temperature, however, has a problem which might be due to the approximations involved or might be due to the fairly restricted knowledge about the Coulomb pseudopotential μ^*.

The authors thank Dr. Reichardt, Dr. Pintschovius, and Dr. Schweiss for many helpful discussions.

[1] J. Nagamatsu, N. Nakagawa, T. Muranaka, Y. Zenitani, and J. Akimitsu, Nature (London) **410**, 63 (2001).
[2] S. L. Bud'ko, G. Lapertot, C. Petrovic, C. E. Cunningham, N. Anderson, and P. C. Canfield, Phys. Rev. Lett. **86**, 1877 (2001).
[3] D. K. Finnemore, J. E. Ostenson, S. L. Bud'ko, G. Lapertot, and P. C. Canfield, Phys. Rev. Lett. **86**, 2420 (2001).
[4] G. Rubio-Bollinger, H. Suderow, and S. Viera, cond-mat/0102242.
[5] B. Lorenz, R. L. Meng, and C. W. Chu, cond-mat/0102264.
[6] G. Karapetrov, M. Iavarone, W. K. Kwok, G. W. Crabtree, and D. G. Hinks, Phys. Rev. Lett. **86**, 4374 (2001).
[7] H. Kotegawa, K. Ishida, Y. Kitaoka, T. Muranaka, and J. Akimitsu, cond-mat/0102334.
[8] J. Kortus, I. I. Mazin, K. D. Belashchenko, V. P. Antropov, and L. L. Boyer, Phys. Rev. Lett. **86**, 4656 (2001).
[9] K. D. Belashchenko, M. van Schilfgaarde, and V. P. Antropov, cond-mat/0102290.
[10] J. E. Hirsch, Phys. Lett. A **282**, 392 (2001).
[11] M. Imada, cond-mat/0103006.
[12] J. M. An and W. E. Pickett, Phys. Rev. Lett. **86**, 4366 (2001).
[13] G. Satta, G. Profeta, F. Bernardini, A. Continenza, and S. Massidoka, cond-mat/0102358.
[14] Y. Kong, O. V. Dolgov, O. Jepsen, and O. K. Andersen, cond-mat/0102499.
[15] B. Meyer, C. Elsässer, and M. Fähnle, "FORTRAN90 Program for Mixed-Basis Pseudopotential Calculations for Crystals," Max-Planck-Institut für Metallforschung, Stuttgart (unpublished).
[16] G. Pelg, Ph.D. thesis, Universität Regensburg (unpublished).
[17] K. M. Ho and K.-P. Bohnen, Phys. Rev. B **32**, 3446 (1985).
[18] D. Vanderbilt, Phys. Rev. B **32**, 8412 (1985).
[19] R. Heid and K.-P. Bohnen (to be published).
[20] R. Heid and K.-P. Bohnen, Phys. Rev. B **60**, R3709 (1999).
[21] R. Heid, L. Pintschovius, W. Reichardt, and K.-P. Bohnen, Phys. Rev. B **61**, 12 059 (2000).
[22] G. Bergmann and D. Rainer, Z. Phys. **263**, 59 (1973).
[23] L. Hedin and B. J. Lundqvist, J. Phys. C **4**, 2064 (1971).
[24] N. I. Medvedeva, A. L. Ivanovskii, J. E. Medvedeva, and A. J. Freeman, cond-mat/0103157.
[25] R. Osborn, E. A. Goremychkin, A. J. Kolesmikov, and D. G. Hinks, cond-mat/0103064.
[26] Taku J. Sato, Kaoru Shibata, and Yoshihiko Takano, cond-mat/0102468.
[27] K. Prassides, Y. Iwasa, T. Ito, Dam H. Chui, K. Uehara, E. Nishibori, M. Takata, S. Sakata, Y. Ohishi, O. Shimomura, T. Muranaka, and J. Akimitsu, cond-mat/0102507.
[28] R. Bauer, A. Schmid, P. Pavone, and D. Strauch, Phys. Rev. B **57**, 11 276 (1998).
[29] J. Schrieffer, *Theory of Superconductivity* (Benjamin, New York, 1964).
[30] K. Voelker, V. J. Anisimov, and T. M. Rice, cond-mat/0103082.
[31] R. W. G. Wyckoff, *Crystal Structures* (Wiley, New York, 1965), Vol. 1.
[32] *Metals: Phonon States, Electron States and Fermi Surfaces,* edited by K.-H. Hellwege and J. L. Olsen, Landolt-Börnstein, New Series, Group 3, Vol. 13a (Springer, Berlin, 1981).